Available online at www.sciencedirect.com
ScienceDirect
Spectrochimica Acta Part A 66 (2007) 626–636
SPECTROCHIMICA ACTA PART A
www.elsevier.com/locate/saa

Vibrational assignment and structure of trifluorobenzoylacetone A density functional theoretical study

Sayyed Faramarz Tayyari [a,*], Mohammad Vakili [a], Abdo-Reza Nekoei [a], Hedayat Rahemi [b], Yan Alexander Wang [c]

[a] *Department of Chemistry, University of Ferdowsi, Mashhad 91775-1436, Iran*
[b] *Department of Chemistry, University of Urmia, Urmia 57159-165, Iran*
[c] *Department of Chemistry, University of British Columbia, Vancouver, BC V6T 1Z1, Canada*

Received 23 February 2006; received in revised form 31 March 2006; accepted 3 April 2006

Abstract

Molecular structure and vibrational frequencies of 4,4,4-trifluoro-1-phenyl-1,3-butanedione, known as trifluorobenzoylacetone (TFBA), have been investigated by means of density functional theory (DFT) calculations. The results were compared with those of benzoylacetone (BA), acetylacetone (AA), and trifluoroacetylacetone (TFAA). Comparing the calculated and experimental band frequencies and intensities suggests coexisting of both stable *cis*-enol conformers in comparable proportions in the sample. The energy difference between the two stable chelated enol forms is negligible, 0.96 kcal/mol, calculated at B3LYP/6-311++G** level of theory. The molecular stability and the hydrogen bond strength were investigated by applying the natural bond orbital (NBO) theory and geometry calculations. The theoretical calculations and spectroscopic results indicate that the hydrogen bond strength of TFBA is between those of TFAA and AA, considerably weaker than that of BA.

Keywords: Trifluorobenzoylacetone; Intramolecular hydrogen bond; Vibrational spectra; Density Functional Theory; NBO

1. Introduction

It is well known that the *cis*-enol form of β-diketones is characterized by a strong intramolecular hydrogen bond [1–4]. The simplest members of this class of compounds are malonaldehyde (MA) and acetylacetone (AA), which have been the subject of many theoretical and experimental studies [5–13]. IR, Raman, NMR, X-ray, neutron, and electron diffraction studies on AA and its derivatives [13–28] indicate that substitution of the methyl groups of AA has a drastic effect on both the position of keto-enol equilibrium and the strength of the intramolecular hydrogen bond. It is well known that the electron-withdrawing substitutes, such as fluorine atom, increase the enol content of β-diketones and decrease the hydrogen bond strength [13,15]. By means of vibrational spectroscopy [23–24], the following trend in hydrogen bond strength has been obtained:

BA > AA > TFAA > HFAA (hexafluoroacetylacetone)

These results are in line with the observation of an increase in proton chemical shift of enolated proton, δOH's (in CCl_4) for HFAA, TFAA, TFBA, AA, and BA are 13.0, 14.2, 15.06, 15.4, and 16.2 ppm, respectively [22].

BA and TFBA can be considered as representative examples of chemically asymmetric β-diketone with different substitution at β-positions. TFBA completely exists in the enol form, even in the $CDCl_3$ solution, whereas BA exhibit 9 and 2% keto form in the $CDCl_3$ and CCl_4 solutions, respectively [29].

The structure and vibrational spectra of BA have been the subject of a few investigations, which support the existence of a strong intramolecular hydrogen bond of chelating nature [23–28]. However, to the best of our knowledge, the TFBA structure and vibrational spectra, theoretically or experimentally, were not described earlier.

The aim of the present paper is to predict the structure and vibrational spectra (harmonic wave numbers, and relative

* Corresponding author. Tel.: +98 511 8780216; fax: +98 511 8438032.
E-mail address: Tayyari@ferdowsi.um.ac.ir (S.F. Tayyari).

1386-1425/$ – see front matter © 2006 Elsevier B.V. All rights reserved.
doi:10.1016/j.saa.2006.04.002

intensities for Raman and IR spectra) of TFBA by means of density functional theory (DFT) levels. The calculated geometrical parameters for TFBA are compared with those of BA and TFAA to obtain a clear understanding of the substitution effects of methyl groups of AA with CF_3 and phenyl groups on the structure and hydrogen bond strength of an asymmetric system. The calculated harmonic force constants of TFBA were used for predicting the Raman and IR spectra of deuterated analogue. The calculated vibrational frequencies and band assignment are compared with those observed experimentally.

2. Experimental

TFBA was obtained from Aldrich Chemical Co. D_2TFBA solution in CCl_4 was readily prepared by exchange with D_2O. The crystalline D_2TFBA was prepared from CCl_4 solution, which was dried over anhydrous Na_2SO_4 followed by removing the organic layer under reduced pressure. Solutions of TFBA and D_2TFBA were made with a constant mole ratio of 1 mol of solute to about 20 mol of solvent.

The mid-IR spectra of TFBA and D_2TFBA were recorded by using Bomem MB-154 Fourier Transform Spectrophotometer in the region 500–4000 cm^{-1} in KBr pellet and in CCl_4/CS_2 solution. The spectra were collected with a resolution of 2 cm^{-1} by coadding the results of 16 scans.

The Far-IR spectra in the region 600–50 cm^{-1} were obtained using a Thermo Nicolet NEXUS 870 FT-IR spectrometer equipped with DTGS/polyethylene detector and a solid substrate beam splitter. The spectra were collected with a resolution of 4 cm^{-1} by coadding the results of 128 scans.

The Raman spectra were collected employing a 180° back scattering geometry and a Bomem MB-154 Fourier Transform Raman spectrometer. The Raman spectrometer was equipped with a ZnSe beam splitter and a TE cooled InGaAs detector. Rayleigh filtering was afforded by two sets of two Holographic technology filters. Laser power at the sample was 200 MW. The spectra were collected with a resolution of 2 cm^{-1} by coadding the results of 250 scans.

3. Method of analysis

Geometrical calculations were performed using GAUSSIAN 03 Version B05 [30] and NBO 5.0 [31] programs. Geometries of the *cis*-enol forms of TFBA are fully optimized with hybrid density functional B3LYP [32,33] using 6-31G** and 6-311++G** basis sets. The vibrational frequencies were calculated at B3LYP/6-311G** level of theory. Orbital populations and Wiberg bond orders [34] were calculated with NBO 3.0 program implemented in GAUSSIAN 03. The second order interaction energies (E^2) [35] were performed at the B3LYP/6-311G** level using NBO 5.0 program, which applied the wave function information file generated by earlier version of NBO (3.0).

The assignments of the experimental frequencies are based on the observed band frequencies and intensity changes in the infrared and Raman spectra of the deuterated species and confirmed by establishing one to one correlation between observed and theoretically calculated frequencies.

4. Results and discussion

4.1. Molecular geometry

A β-dicarbonyl compound predominantly exists as conjugated *cis*-enol form, stabilized by an intramolecular hydrogen bond. Two different isomeric *cis*-enol forms are distinguishable in the case of unsymmetrical β-dicarbonyl compound, an interconversion occurs by transfer of an enol proton from one oxygen atom to the other.

From the theoretical point of view, 16 enol conformations can be drawn for TFBA molecule, which only two of them are engaged in a six-member ring intramolecular hydrogen bonded system. The structures of these two conformers and their *trans*-enol forms, open structures, along with atom numbering of the system are shown in Fig. 1.

For TFBA, two possible isomers characterized by the position of the phenyl group, which can be attached at C_2 (i.e. adjacent to C=O bond) or at C_4, are conceivable. They are labeled as 2TFBA and 4TFBA, respectively.

The full optimized structural parameters of both *cis*-enol forms of TFBA are collected in Table 1. For comparison, the corresponding geometrical parameters of BA and TFAA, calculated at the same level of calculation, are also given in Table 1.

The hydrogen bond strength, E_{HB}, (the energy difference between chelated and open structures), OH/OD stretching and OH/OD out-of-plane bending frequencies, proton chemical shift of the enolated proton, and the calculated O···O distance for TFBA, BA, AA, and TFAA are compared in Table 2.

According to the calculations, 2TFBA has almost *Cs* symmetry. However, the phenyl ring in 4TFBA shows a few degrees deviation from coplanarity with the enol ring. These results reveal that in both tautomers, phenyl group strongly takes part in the conjugation with the π-electrons of the enol ring.

The averaged O···O distance in TFBA, calculated at B3LYP/6-311++G**, is 0.016 Å longer than that in BA while is 0.013 and 0.026 Å shorter than the corresponding values in AA and TFAA, respectively. These results are well supported by the NMR proton chemical shifts of 16.2, 15.4, 15.06, and 14.2 ppm [22] for BA, AA, TFBA, and TFAA, respectively (see Table 2).

As it is shown in Table 1, in 4TFBA the C=C bond length is considerably longer and the C–C bond length is considerably shorter than those in 2TFBA. These results could be explained by considering the electron withdrawing nature of CF_3 group, which in the case of 4TFBA causes an electron migration from C=C bond towards C–C bond, while in the case of 2TFBA this electron migration is reversed. Similar behavior is reported for TFAA [13]. On the other hand, the C=O bond length in 2TFBA (1.247 Å) is considerably longer than that in 4TFAA (1.240 Å). This result could be explained by considering that the phenyl group in 2TFBA is conjugated only with the C=O group.

Table 1 also shows that the C–CF_3 bond length in TFBA is 1.536 Å, in compare with the C–CH_3 bond length in BA (1.503 Å [29]), is considerably increased. Electrostatic effects can rationalize this lengthening of the C–C bond, qualitatively if we

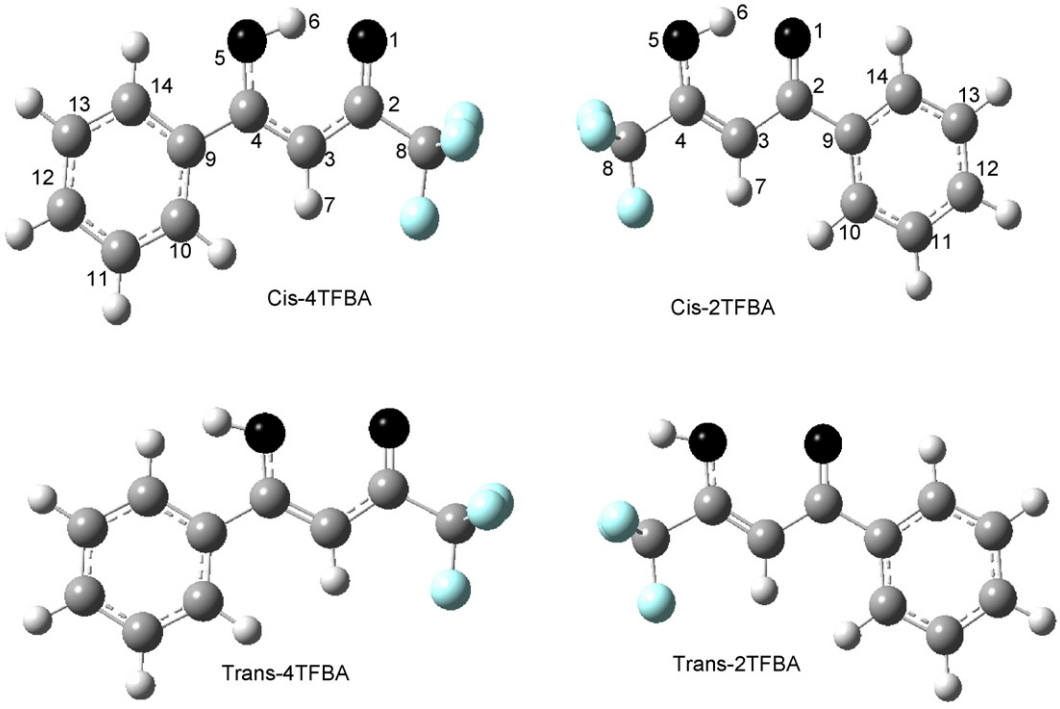

Fig. 1. Numbering system and the structures of *cis*- and *trans*-enol forms of 2TFBA and 4TFBA.

assume that the small but negative net charge on the CH_3 carbon atoms becomes positive upon fluorination. In this picture, the attractive interaction ($C^{+\delta}$–$C^{-\delta}$) in BA becomes repulsive ($C^{+\delta}$–$C^{+\delta}$) if fluorination occurs on terminal carbon atom.

According to the data depicted in Table 2, the following trend in the hydrogen bond strength is concluded:

TFAA < TFBA < AA < BA

This trend suggests that the electron-withdrawing groups, such as CF_3, decrease the intramolecular hydrogen bond strength and the π-systems, such as phenyl group, increase the H-bond strength.

As it is indicated in Table 2, the hydrogen bond energy, E_{HB}, difference between 2TFBA and 4TFBA is about 2.3 kcal/mol. This difference in hydrogen bond strength could be explained as follows:

1- One part of this energy difference originates from intramolecular hydrogen bonding between CF_3 and OH groups in 2TFBA *trans* conformer. This effect decreases the energy of open structure, therefore, results in lower E_{HB}.
2- The steric effect of phenyl ring in the *trans*-enol conformer of 4TFBA with the enolated proton is a factor which increases the energy of the *trans*-enol form and, consequently, increases E_{HB}. This steric effect causes that the dihedral angle between phenyl and enol rings in the *trans* conformer of 4TFAA to deviate considerably from coplanarity ($\Phi = 37.7$) [13].

The energy difference between 2TFBA and 4TFBA tautomers is only 0.96 kcal/mol (see footnote of Table 2), which suggests probable coexisting of both *cis*-enol tautomers at least in the gas phase.

4.2. NBO analysis

4.2.1. Bond order

The calculated Wiberg bond orders [34] for 2TFBA, 4TFBA, 2BA, and 4BA, for comparison, are collected in Table 3. This table shows that the C=O bond order in 2TFBA is significantly less than that in 4TFBA. This result is explainable if we notice that in 2TFBA the phenyl and C=O groups are adjacent, therefore, a conjugation between C=O and phenyl is expected, however, in 4TFBA there is a conjugation between the phenyl group and the C=C bond, which affects the C=C bond order.

Comparing the C–C and C=C bond orders of 4TFBA with those of 2TFBA shows that with considering the electron withdrawing nature of CF_3 group, in 4TFBA the C=C bond order is considerably smaller and C–C bond order is considerably larger than those of 2TFBA (same as TFAA [13]). This discussion could also be used for substitution of CF_3 group for CH_3 in BA (compare these bond orders for TFBA and BA conformers).

It is noteworthy that the O–H bond order correlates with the calculated O···O distance, by increasing the hydrogen bond strength, reducing the O···O distance, the O–H bond order decreases.

4.2.2. Electron delocalization

Delocalization of electron density between occupied Lewis-type (bond or lone pair) NBO orbitals and formally unoccupied (antibond or Rydberg) non-Lewis NBO orbitals corresponds to a stabilizing donor–acceptor interaction. The energy of these

Table 1
Comparison of calculated structural parameters for TFBA, BA, and TFAA[a]

	2TFBA		4TFBA		2BA [b]	4BA[b]	2TFAA [c]	4TFAA [c]
	A	B	A	B	B	B	B	B
Bond lengths (Å)								
O···O	2.499	2.525	2.508	2.54	2.52	2.513	2.566	2.55
C_4—O_5	1.318	1.318	1.323	1.322	1.324	1.326	1.32	1.318
C_2—O_1	1.256	1.247	1.25	1.24	1.252	1.25	1.237	1.24
O_5—H_6	1.017	1.006	1.014	1.001	1.006	1.01	0.997	1.002
O_1···H_6	1.568	1.621	1.572	1.63	1.604	1.585	1.672	1.654
C_4—C_8/C_2—C_8[d]	1.519	1.522	1.54	1.549	1.496	1.511	1.492	1.522
C_4—C_3	1.363	1.358	1.389	1.386	1.372	1.378	1.378	1.367
C_3—C_2	1.452	1.456	1.42	1.42	1.443	1.439	1.426	1.457
C_2—C_9/C_4—C_9	1.489	1.49	1.474	1.473	1.495	1.478	1.55	1.506
C_3—H_7	1.078	1.077	1.078	1.076	1.078	1.079	1.078	1.079
Bond angles (°)								
$C_2C_3C_4$	118.7	119.2	118.9	119.5	120.6	119.2	119.5	119.36
$C_4C_3H_7$	118.9	118.8	119.6	119.6	118.3	120.2	119.9	120.67
$C_2C_3H_7$	122.4	122	121.5	120.9	121.1	120.6		
$O_1C_2C_3$	119.8	119.7	124.9	120.5	120.5	121.7	113.9	121.1
$O_1C_2C_9$/$O_5C_4C_9$[d]	119	119.4	114.9	114.7	118.6	114.6	125.1	120.74
$C_3C_2C_9$/$C_3C_4C_9$	121.3	120.9	124.9	124.7	120.9	124.8		
$C_2C_9C_{10}$/$C_4C_9C_{10}$	123.1	123.1	121.9	121.8	123.1	121.9		
$C_2C_9C_{14}$/$C_4C_9C_{14}$	117.9	117.9	119.1	119.2	118.1	119.3	107.6	105.7
$C_4O_5H_6$	104	105.1	98.2	98.3	105.8	106.1		
$C_2O_1H_6$	103.1	103.6	106.5	107.6	101.9	100.5	146.8	146.46
$O_1H_6O_5$	149.6	147	151.2	148.8	148.9	150.5		
$C_4C_8F_{22}$	110.6	110.9	110	110.1	111.6	112.4		
$C_4C_8F_{21}$	110.6	110.9	110.6	111	109.7	109.6		
$C_4C_8F_{20}$	111.5	111.7	112.2	112.5	109.2	108.8		
$O_5C_4C_8$/$O_1C_2C_8$	112.7	112.3	116.1	116.1	113.8	119.1	113.9	112.3
$O_5C_4C_3$/$O_1C_2C_3$	124.9	125.4	124.9	125.3	122.2	121.7	122.2	125.14
$C_3C_4C_8$/$C_3C_2C_8$	122.4	122.3	118.9	118.6	123.9	117.6		
Φ	−0.7	−0.16	2.8	5.1	8.9	12.6		

[a] All calculations are performed at B3LYP level of theory using 6-31G** (A) and 6-311++G** (B) basis sets; Φ, dihedral angle between phenyl and enol rings.
[b] Data from Ref. [28].
[c] Data from Ref. [13].
[d] The first and second geometrical parameters given in the first column are for 2TFBA and 4TFBA conformers, respectively.

interactions can be estimated by the second order perturbation theory [35].

Table 4 lists the calculated second order interaction energies E^2 between the donor–acceptor orbitals in TFBA, BA, and AA. According to this table, there is no significant difference between the interaction energies of the compared species, except the interaction energies between the C=O and C=C in 2TFBA and 4TFBA together or with phenyl group. Table 4 indicates

Table 2
Comparison between several properties related to the hydrogen bond strength for TFBA, BA, and AA[a]

	E_{HB}	νOH	νOD	γOH	δOH	γOD	R
2TFAA[b]	13.6	2900	2120	893	14.2	650	2.566
4TFAA[b]	13.1						2.550
2TFBA	13.9[c]	2870	2090	890	15.06	680	2.525
4TFBA	16.2[c]						2.540
2BA[d]	16.4	2650	1960	960	16.2	720	2.520
4BA[d]	15.8						2.513
AA[e]	15.9	2800	2020	952	15.4	649	2.544[b]

[a] E_{HB}, hydrogen bond energy (energy difference between *cis* and *trans* conformers), in kcal/mol, calculated at B3lyp/6-311++G** level; δ, proton chemical shift (in ppm); ν and γ are stretching and out of plane bending frequencies, in cm^{-1}; R, O···O distance, in Å.
[b] Data from Ref. [13].
[c] Absolute electronic energies of 2TFBA and 4TFBA are −835.5037795 and −835.5022469 Hartrees, respectively (calculated at 6-311++G** level of theory). This gives an energy difference of about 0.96 kcal/mol between two tautomers of TFBA.
[d] Data from Ref. [28].
[e] Data from Ref. [6].

Table 3
Selected Wiberg bond orders of BA and TFBA calculated at B3LYP/6-311G** level

Bond	2BA	4BA	2TFBA	4TFBA
O–H	0.6205	0.6144	0.6207	0.6240
C–O	1.1670	1.1520	1.1671	1.1711
C=C	1.5403	1.5095	1.6091	1.4480
C–C	1.1870	1.2003	1.1393	1.2615
C=O	1.5309	1.5673	1.5606	1.5710

that πC=C → π*C=O for 2TFBA is about 6 kcal/mol less than that for BA and AA while the corresponding interaction for 4TFBA is about 6 kcal/mol more than that for BA and AA. These results could be explained if we consider the electron-withdrawing nature of the CF_3 group. In 4TFBA the CF_3 group is adjacent to the C–C bond and cause electron migration from C=C towards C–C and helps more electron delocalization in the enol ring. In the case of 2TFBA the CF_3 group is adjacent to the C=C bond group and by removing electrons from this band reduces the resonance between C=C and C=O bonds.

The interaction between the π orbitals of phenyl group and π* of the adjacent double bond in the enol ring is relatively large, about 23 kcal/mol. Therefore, stabilization through resonance with the phenyl group is expected. This may explain the almost coplanarity of the phenyl and enol rings in TFBA. The calculated dihedral angle between phenyl and enol rings, on average, is about 2.5°, which indicates that in both TFBA tautomers the coplanarity is even better than that in BA (dihedral angle10.8°). This is consistent with the corresponding E^2 in BA and TFBA (Table 4).

It is noteworthy that the E^2 of LP(2)O_1 → σ* (O–H) could be well correlated to the O···O distance. The high value of this energy, about 28 kcal/mol, indicates that this interaction plays an important role in stabilization of the *cis*-enol form of β-diketones.

4.2.3. Charge analysis

The charge distribution calculated by the NBO method for optimized geometries of TFBA and BA chelated tautomers are tabulated in Table 5. As Table 5 indicates, substitution of CF_3 group for CH_3 in BA considerably reduces the charge distribution over ring atoms, which indicates the strong electron withdrawing nature of the CF_3 group.

Table 5
Selected natural charges (e) for optimized *cis*-enol TFBA and BA[a]

Atom	2TFBA	4TFBA	2BA[b]	4BA[b]
O_1	−0.636	−0.61	−0.655	−0.642
O_5	−0.634	−0.646	−0.658	−0.663
C_2	0.534	0.426	0.525	0.547
C_3	−0.413	−0.447	−0.455	−0.449
C_4	0.351	0.488	0.49	0.463
H_6	0.502	0.501	0.496	0.496

[a] All calculation at B3LYP/6-311G** level of theory.
[b] Data from Ref. [28].

The natural charges over O_1 and O_5 in 2TFBA are higher and lower than those in the corresponding atoms in 4TFBA, respectively. These results could be used to explain the shorter O···O distance in 2TFBA than that in 4TFBA. More negative O atom of C=O group results in formation of stronger hydrogen bond while more negative O atom of the hydroxyl group leads to weaker acidic group, therefore, gives weaker hydrogen bond.

4.3. The interpretation of the vibrational spectra

The assignments of the experimental frequencies are based on the observed band frequencies and intensity changes in the infrared and Raman spectra of the deuterated species confirmed by establishing one to one correlation between observed and theoretically calculated frequencies.

The calculated vibrational band frequencies and their approximate assignments for 2TFBA, 4TFBA, and for the corresponding deuterated analogous along with the observed infrared and Raman frequencies are listed in Tables 6 and 7, respectively. Assignments for vibrational modes of the phenyl group are given in Wilson's notation [36]. The IR and Raman spectra of TFBA and D_2TFBA are shown in Figs. 2 and 3, respectively.

Lorentzian function has been utilized for deconvolution of the IR and Raman spectra of TFBA in the 800–1700 cm^{-1} region

Table 4
Selected second order perturbation energies E^2 (donor → acceptor) for TFBA, BA, and AA[a]

Donor	Type	Acceptor	Type	2-BA	4-BA	AA	2TFBA	4TFBA
C=C	π	C=O	π*	32.4	33.4	32.5	26.0	39.7
C_9–C_{14}	π	C=C	π*	–	19.6	–	–	22.7
C_9–C_{10}	π	C=O	π*	21.9	–	–	23.4	–
O_5	CR(1)	C_4	RY*(1)	3.9	5.9	3.8	5.3	3.3
O_1	CR(1)	C_2	RY*(1)	5.2	5.9	5.9	5.3	5.5
O_1	LP(1)	C–C	σ*	5.2	5.6	5.3	5	5.2
O_1	LP(2)	C–C	σ*	9.1	9.2	9.8	9.9	9.3
O_1	LP(2)	C_2–$C_{8(9)}$	σ*	16.8	17.4	17.8	16.7	22.5
O_1	LP(2)	O–H	σ*	30.8	32.5	28.1	28.6	27.8
O_5	LP(1)	C=C	σ*	7.2	6.9	7.1	7.6	7.6
O_1	LP(1)	C_2	RY*(1)	10.2	11.9	12.2	10.3	11.1
O_5	LP(2)	C=C	π*	50.4	48	49.8	48.9	49.6
C_3–H_7	σ	C–O	σ*	6.4	6	6.4	7.1	4.5
O–H	σ	C_4–$C_{8(9)}$	σ*	5.9	5.7	5.8	6	5.6

[a] Energy in kcal/mol. Data for BA and AA from Ref. [28].

Table 6
Fundamental band assignment of TFBA (frequencies in cm^{-1})[a]

No.	Theoretical[b]						Experimental			Assignment[c]
	2TFBA			4TFBA			IR, solid	IR, CCl_4	*R*, solid	
	Frequency	I.IR	I.R	Frequency	I.IR	I.R				
1	3265	1	39	3265	2	34	3124(1)	3117,sh	3121, vw	νCH_α
2	3208	5	118	3217	2	91	3080,sh	3087, vw	3080 (12)	2
3	3202	9	103	3202	7	111	3080, sh	3071	3080 (12)	20b
4	3190	21	164	3191	19	183	3069, mw	3068	3070 (9)	20a
5	3180	9	131	3180	8	128	3051, sh	3041	3049, sh	7b
6	3169	0	57	3171	0	55		3037	3026 (1)	13
7	3037	349	99	3051	324	6		2870(vbr)		νOH
8				1674	140	15		1635(20)	1625(7)	ν_aC═C─C═O + δCH + 8b
	1687	497	29					1635	1625	ν_aC═C─C═O + δCH + 8b + δOH
9	1648	75	26	1641	571	448	1602(100)	1605(65)	1600(100)	νsC═C─C═O + 8b + δOH
10				1645	9	324		1602(8)	1600	8a
	1640	18	337					1602	1600	8a + νC═O + δOH
11				1616	129	20	1572(40)	1575(20)	1595(8)	8b + νC═C + δOH + δCH
	1611	33	89				1565(25)	1565(13)	1563(17)	8b + νC═O + δOH
12	1528	5	15	1528	14	40	1493(50)	1494(8)	1500(8)	19a
13				1498	165	14	1470(50)	1474(9)		19b + ν_aC─C═C─O + δOH + δCH
	1484	36	2				1470(50)	1462(10)		ν_aC─C═C─O + 19b + δCH + δOH
14	1470	28	1	1469	89	7		1425(6)		ν_aC─C═C─O + 19b + δCH + δOH
15	1394	107	170	1399	53	29	1345(35)	1336(7)	1350(15)	δOH + ν_sC─C═C─O + 3
								1320(9)		Combination?
16	1355	4	13	1360	2	6	1315(25)	1296(16)	1300(20)	3
17	1338	80	26	1331	40	59	1278(35)	1280(48)	1279(15)	δOH + 14 + νCF_3
18				1316	378	377		1269 (24)		δOH + νC─CF_3 + νC─C + νC─Ph
	1304	792	83				1254(35)	1248(17)	1250(50)	δOH + νC─CF_3 + νC─C + νC─Ph
19	1258	78	73	1263	105	119		1234(10)	1238(25)	νCF_3 + δCH
20	1207	59	6	1212	47	30	1180(32)	1190(20)	1185(15)	9a
21	1193	337	2	1189	255	1	1202(85)	1205(99)		$\nu_a CF_3$
22	1186	2	8	1188	4	10				9b
23	1172	295	4	1170	280	2	1152(25)	1162(100)	1166(15)	$\nu_a CF_3$
24	1140	59	9	1138	114	1	1118(28)	1116(40)	1120(5)	$\nu_s CF_3$ + δCH + νC─O + 18b
25	1108	29	0	1110	67	0	1086(12)	1096(14)		18b
26				1090	110	2	1068(17)	1071(25)	1065(2)	18a + νC─O + δCH + $\nu_s CF_3$
	1070	10	2						1035(1)	18a + νC─C
27	1045	15	25	1048	3	17	1023(14)	1025(4)	1025(9)	18a
28	1021	0	0	1018	0	1	997(6)	1001(5)		5
29	1017	3	45	1017	5	61	997(6)	1001(5)	1000(45)	12
30	997	0	0	993	0	0	975(5)	973(2)	975(2)	17a
31				959	76	1	897(8)	888(7)		γOH
32				951	4	1	934(1)	928(7)	934(2)	17b
31	954	35	0				914(12)	919(5)	916(11)	17b + γOH
32	949	39	1				914(12)	919(5)	916(11)	17b + γOH
33	932	40	15	940	21	22	897(15)	896(br)	900(2)	δCCC
34	862	3	1	858	1	1	846(6)	844(1)*	843(1)	10a
35	842	11	0	831	14	1	815(15)		813(2)	γCH + 10a
36	811	11	3	809	10	3	805(8)	808 (11)*	804(2)	1 + Δ + νC─CF_3 + $\nu_s CF_3$
37	799	63	1	791	68	0	775(35)	771(35)*	781(3)	γCH + 11
38	734	1	0	763	1	0				γCH + γOH
39	717	7	7	724	24	5	716(25)	718(15)	719(11)	$\delta_s CF_3$ + 1 + Δ
40	708	48	1	701	44	1	691(45)	692(30)	697(2)	11
41	697	3	0				679, sh	680, wsh	675(1)	4
				689	0	1	662, w		670(1)	4
42	645	59	2	637	33	4	624(28)	627(19)	625(8)	6b + Δ + $\delta_s CF_3$
43	631	2	6				609(15,sh)		615(8)	6b + Δ + $\delta_s CF_3$
				631	12	5	609(15,sh)		615(8)	6b + Δ
44	581	13	1				583(23)	578 (15)	580(5)	$\delta_a CF_3$ + Δ
				574	21	2	559(15,sh			$\delta_a CF_3$ + Δ
45	516	1	2	515	2	1	517(5,sh)	518(1)		$\delta_a CF_3$
46	489	3	10	483	6	1		475(1)#		15 + δC─C═O
47	455	2	0	459	4	0	458(1)#	461(1)		16b
48	438	2	0	446	0	1	439(5)	435(3)		νO···O + δCF_3

Table 6 (*Continued*)

No.	Theoretical[b]						Experimental			Assignment[c]
	2TFBA			4TFBA			IR, solid	IR, CCl_4	*R*, solid	
	Frequency	I.IR	I.R	Frequency	I.IR	I.R				
49	410	0	0	408	0	0	399(1)	399(1)	400(1)	16a
50	367	2	1	361	3	1	360(5)	354(3)	360(6)	Δ
51	321	7	4	337	3	1	293(2)	303(2)		νO···O + rCF3 + 15
52	302	0	1	284	1	0	238(7)			$\Gamma + \text{JICF}_3$
53	238	2	1	238	2	6	225(9)		228(8)	νO···O
54	216	2	0	218	2	1	208(6,sh)		219(6)	$15 + \delta\text{C—CF}_3$
55	186	0	5				196(4,sh)		186(3)	$10b + \Gamma$
				207	1	3			205(2)	γC—Ph
56	124	3	1	105	1	1	130(6)		127, vw	$\Gamma + \gamma\text{CCF}_3$
57	91	0	1	93	0	1	95(2)			δC—C—Ph
58	82	0	0	89	1	2	73(5)		77(6)	γCPh
59	21	0	3	23	0	1	n.m			$\tau\text{-CF}_3 + \tau$C—Ph
60	13	0	4	13	6	4	n.m		49(12)	$\tau\text{-CF}_3 + \tau$C—Ph

[a] IR, infrared; R, Raman; *ν*, stretching; *δ*, in plane bending; *γ*, out of plane bending; Δ, in plane ring deformation; *Γ*, out of plane ring deformation; v, very; s, strong; m, medium; w, weak; sh, shoulder; *τ*, torsion; n.m., not measured; relative intensities are given in parentheses, *, in CS_2 solution; Ph, phenyl; #, below 500 cm^{-1} has different scale.

[b] Unscaled frequencies calculated at B3LYP level with basis set 6-311G**; I.IR, infrared intensity in KM/Mole; I.R, Raman scattering activities in A^4/AMU.

[c] Wilson's notation [36] for phenyl vibrational modes.

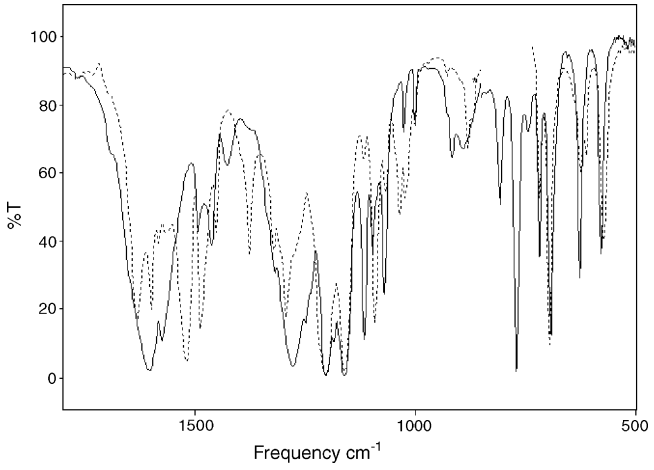

Fig. 2. The IR spectra of TFBA (—) and D_2TFBA (···) in CCl_4 and CS_2 (*) solutions.

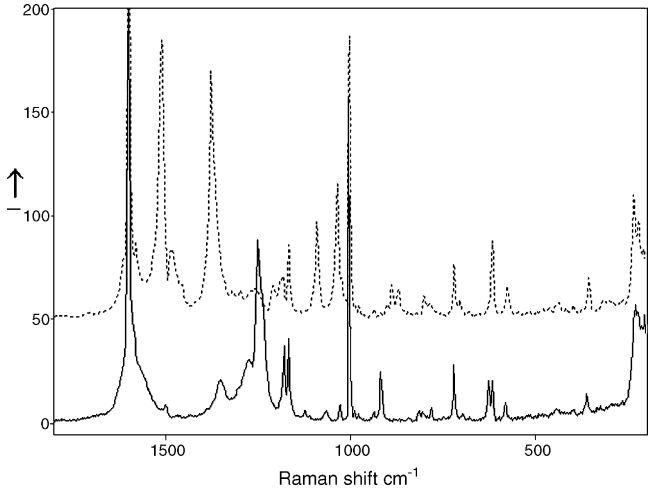

Fig. 3. The Raman Spectra of TFBA (—) and D_2TFBA (···) in the solid state.

and the deconvoluted spectra are shown in Figs. 4 and 5, respectively.

The calculated frequencies are slightly higher than the observed values for the majority of the normal modes. In addition to the error of the theoretical method used, the difference between the computed and experiment frequencies may be due to many different factors that are usually not even considered in the theory, such as anharmonicity, Fermi resonance, solvent effects, etc.

4.3.1. CH stretching modes

Upon deuteration, the weak band at 3117 cm^{-1} disappears and a new band at 2323 cm^{-1} appears which certainly can be attributed to the CH_α stretching. This is consistent with the calculated results, which assigns the highest frequency to this mode.

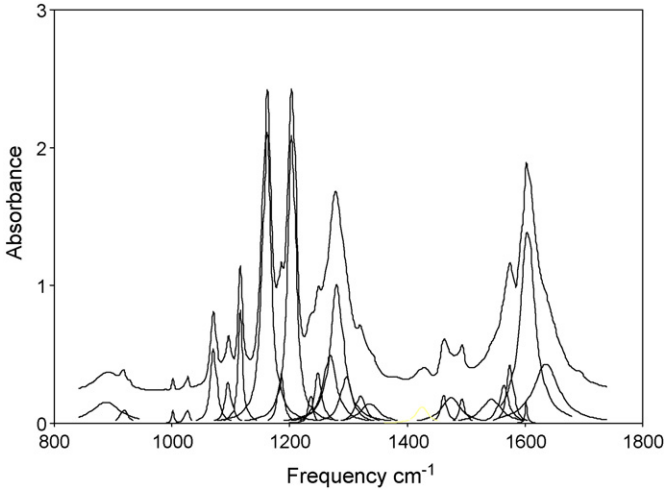

Fig. 4. Deconvoluted infrared spectrum of TFBA in CCl_4 solution in the 800–1700 cm^{-1} region.

Table 7
Comparison of calculated and observed spectra of D_2TFBA (frequencies in cm^{-1})[a]

No.	Theoretical[b]						Experimental			Assignment[c]
	2TFBA			4TFBA						
	Frequency	I.IR	I.R	Frequency	I.IR	I.R	IR, Solid	IR, CCl_4	R, Solid	
1	3208	5	124	3217	2	92		3089 (2)	3093(2,sh)	2
2	3202	8	105	3203	7	116		3089	3093(2,sh)	20b
3	3190	21	166	3191	19	184		3072(4)	3075(7)	20a
4	3180	9	130	3181	8	128	3067(1)	3068, sh	3064(5)	7b
5	3169	0	55	3171	0	54		3045(2)		13
6	2411	2	11	2412	3	10	2312(5)	2323(3)	2316(1)	νCD
7	2220	230	30	2235	261	3	2088(6)	2092(5)		νOD
8	1670	347	8	1664	142	14		1633(35)	1616(10,sh)	ν_aC═C─C═O + 8b
9	1642	79	204	1644	25	435	1601(35)	1601(28)	1599(100)	8a
10				1619	26	42	1570(15,sh)	1568(12)	1579(10)	8b + νC═O
	1622	65	22				1580(17,sh)	1583(10)	1579(10)	8b + νC═C
11				1546	589	455	1515(55)	1520(59)	1509(48)	ν_sC═C─C═O + 19a + δOD
	1575	69	398				1527(45,sh)	1530(59,sh)	1525(13,sh)	ν_sC═C─C═O + 19a + δOD
12	1525	2	29	1521	317	29	1489(20,br)	1490(38)	1481(11)	19a + ν_sC═C─C═O
13				1483	55	12	1454(13)	1453(11)	1453(4)	19a
	1478	18	31				1454	1453	1453	19b + ν_aC─C═C─O
14				1403	68	2	1376(30)	1379(10)	1375(44)	ν_aO─C═C─C + 3 + νC═O + δOD
	1430	25	20				1390(20,sh)	1390(10)		ν_aO─C═C─C + 3 + νC═O + δOD
15				1375	44	336	1343(18)		1340(2)	ν_sC─C═C─O + 20a + νC─CF_3
	1356	34	3	1358	1	9	1323(15)	1320(7)	1317(1)	3
16	1342	181	13				1299(22)	1295(34)	1295(1)	14
17				1326	40	3				14
	1314	575	20				1260(25)	1265(21)	1260(7,vbr)	νC─CF_3 + νaC─C─ph + δOD + 14
							1235(vw)	1235(vw)		625 × 2
18				1224	314	7	1204(100)	1212(70)	1207(6)	20a + ν_sC─C═C─O + δOD + νC─CF_3
	1219	175	22				1204(100)	1203(100)	1207(6)	20a + ν_sC─C═C─O + νCF_3 + νC─CF_3
									1187(2)	615 + 574 = 1189?
19	1207	15	5	1212	3	14	1182(m)		1182(3)	9a
20	1194	236	2	1188	238	2	1150(s)	1161(73)	1166(10)	νaCF_3 + 9b
21	1185	0	9	1188	18	11			1157(3,sh)	9b
22	1171	288	11	1169	279	2	1121(11)	1118(2)		νaCF_3
23	1123	177	110	1127	147	99	1089(18)	1092(29)	1090(16)	δOD + 18a + $\nu_s$$CF_3$
24	1111	10	0	1114	15	0	1065(15)	1068(6)		18b
25	1065	59	25	1072	104	41	1035(5)	1036(8)	1036(23)	δOD + ν_sC–C─C + 18a
26	1042	48	8	1047	8	9	1021(9)	1023(8)	1026(sh)	18a + δOD + ν_sC–C─C
27	1021	0	1	1017	0	1				5
28	1018	2	44	1017	5	56		1003(2)	1000(51)	12
29	997	0	0	992	0	0	972(1)		975(3)	17a
30	951	1	1	951	1	2	933(1)	928(1)	933(2)	17b
31				897	12	5	900(1)	900(1)	900(1)	δCD + δC─C─C
	899	10	4				900(1)	900(vw)	900(1)	δCD + 1 + Δ
32				893	22	14	884(3)	882(8)	887(4)	δCD + δC─C─C + δOD
	872	10	7				870(2)	870(2)	870(3)	δCD + δC─C─C + δOD
33	859	0	1	855	0	5		*	841(1)	10a
34				824	7	1	801(2)	*	800(3)	11 + Γ
	835	4	1				815(2)	*	817(1)	11 + Γ
35	800	4	2	796	5	4	801(2)	*	800(3)	1 + Δ + νC─CF_3 + $\nu_s$$CF_3$
36				783	62	0	780(5,sh)	*	783(1)	11 + Γ
	767	75	0				770(5)		772(1)	11 + Γ
37				723	26	5	762(5)	*	760(1)	$\delta_s$$CF_3$ + 1 + Δ
	711	41	2				717(5)	719(12)	719(10)	1
38	711	8	7	709	76	2	695(42)	697(45)	702(3)	11
39				703	1	0	681(25,sh)	680(1,sh)	680(1)	γOD + 4
	697	2	1				681(25,sh)	680(1,sh)	680(1)	4

Table 7 (*Continued*)

No.	Theoretical[b]						Experimental			Assignment[c]
	2TFBA			4TFBA						
	Frequency	I.IR	I.R	Frequency	I.IR	I.R	IR, Solid	IR, CCl_4	R, Solid	
40				676	8	1	670(10,sh)			γOD + 4
	682	25	0				665(7,sh)			γOD + γCD
41				625	38	2	612(2)	612(9)	615(14)	6b + Δ + $\delta_s CF_2$
	641	53	2				640(14)	640(2,sh)		6b + Δ + $\delta_s CF_3$
42	630	9	6	634	5	7	622(14)	625(9)	622(2,sh)	6b + Δ
43				587	10	0	611(13)	613(6)	615(12)	γCD
	590	11	1				611(13)	613(6)	615(12)	γCD + γOD
44	578	11	1	570	21	2	575(10)	571(17)	574(6)	Δ + $\delta_a CF_3$
45	513	0	2	513	1	1	516(1)	518(1)		$\delta_a CF_3$
46				474	5	1	480(3)	486(1)		15 + νO···O
	482	3	10				486(2)	486(1)		Δ + δC—Ph
47	454	3	0	456	5	0	442(2)		437(3)	16b
48	432	2	1	441	0	1	432(4)	432(1)	437(3)	νO···O + $\delta_s CF_3$
49				407	0	0	400(1)	401(1)		16a
	410	0	0				410(1)		412(1)	16a
50				356	3	2	353(2)	354(1)	353(7)	Δ
	366	2	1				353(2)	354(1)	353(7)	Δ + 15
51	310	7	5	330	3	0	313(2)	314(1)		νO···O + ρCF_3 + 15
52				282	1	0	274(1)	274(1)		γC—CF_3
	299	0	1						300(2)	Γ + JICF_3
53	236	2	1	236	2	5	235(1)	234(1)	233(11)	νO···O
54	215	2	0	217	2	1	222(1)	222(1)	219(4)	15 + δC—CF_3
55	184	0	5	205	1	3	n.m	n.m		10b + Γ
56	122	3	1	104	1	1	n.m	n.m		γC—CF_3
57	90	0	1	92	0	1	n.m	n.m		δC—Ph
58	80	0	1	87	1	2	n.m	n.m	75(5)	γC—Ph
59	21	0	3	23	0	2	n.m	n.m	49(8)	τ-CF_3 + τC—Ph
60	13	0	5	13	0	6	n.m	n.m	n.m	τ-CF_3 + τC—Ph

[a] IR, infrared; R, Raman; ν, stretching; δ, in plane bending; γ, out of plane bending; Δ, in plane ring deformation; Γ, out of plane ring deformation; v, very; s, strong; m, medium; w, weak; sh, shoulder; τ, torsion; n.m., not measured; relative intensities are given in parentheses, *, in CS_2 solution; Ph, phenyl; #, below 500 cm^{-1} has different scale.

[b] Unscaled frequencies calculated at B3LYP level with basis set 6-311G**; I.IR, infrared intensity in KM/Mole; I.R, Raman scattering activities in A^4/AMU.

[c] Wilson's notation [36] for phenyl vibrational modes.

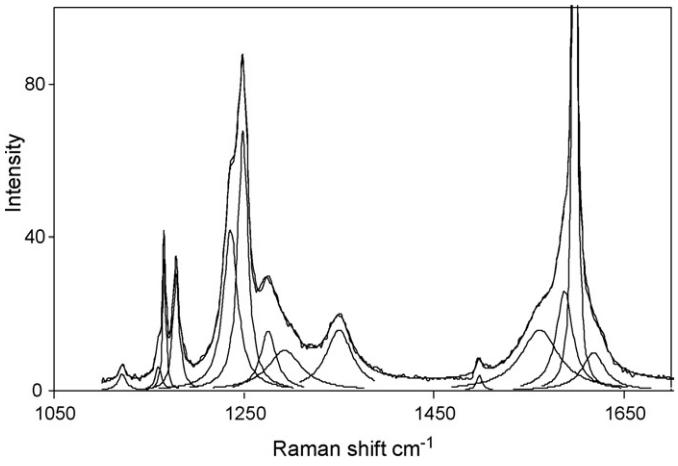

Fig. 5. Deconvoluted Raman spectrum of TFBA in the solid state in the 800–1700 cm^{-1} region.

In the mono-substituted benzene ring, the vibrational modes 2, 20a, and 20b are expected to be observed in the 3105–3035 cm^{-1} region [37]. By considering the computed results, five bands in the 3090–3030 cm^{-1} range are assigned to the CH stretching of the phenyl group.

4.3.2. OH stretching mode

The position and the shape of the OH stretching band are closely related to the shape of the potential energy function governing the motion of the proton. For the enol form of β-diketones, determination of the precise position of this band is difficult because it appears as a very weak band with several hundred cm^{-1} bandwidth at half height [23,24,28] and overlaid by overtones. The intensity and broadness of this band are depended on the strength of the intramolecular hydrogen bond. Upon increasing the hydrogen bond strength, its intensity decreases while its broadness increases [24,38,39].

This band in IR spectrum of TFBA is centered at about 2870 cm^{-1} with a bandwidth at half height of about 425 cm^{-1}. Upon deuteration, this band disappears and a new band with

considerably narrower band width appears at 2092 cm^{-1}, which indicates a νOH/νOD ratio of 1.37. The higher frequencies of νOH and νOD and the higher ratio of νOH/νOD for TFBA in comparison with the corresponding values for AA and BA confirms weaker hydrogen bond in TFBA compared with that in AA and BA. The νOH band in AA [6] and BA [28] appears at 2800 and 2650 cm^{-1}, respectively.

4.3.3. 1700–1000 cm^{-1} region

In this region, we expect to observe the band frequencies related to the C–C, C=C, C–O, C=O stretching, and OH and CH in-plane bending movements of the enol ring, the CF_3 and C–C stretching and the C–H in-plane bending of the phenyl group.

The infrared spectra of BA [28], AA [6], and several other β-diketones [23,24], apparently show only one broad band in the C=O and C=C region. This band in the CCl_4 solution of TFBA appears at about 1600 cm^{-1}. Deconvoluted infrared spectrum of TFBA in this region indicates five bands at 1635, 1605, 1602, 1575, and 1565 cm^{-1}. The weak and sharp band at 1602 cm^{-1}, which is not affected by deuteration, is clearly assigned to the C–C stretching of the phenyl group (8a). The corresponding Raman band appears as a very strong band at 1599 cm^{-1} in the solid state of light and deuterated compounds, which confirms the assignment. According to the theoretical calculations, the medium intensity IR band at 1635 cm^{-1} is caused by asymmetric C=C–C=O stretching which is slightly coupled to 8b, δOH and δCH. Upon deuteration this band moves about 10 cm^{-1} towards lower frequencies. This frequency shift is in excellent agreement with the calculation results. The corresponding band in TFAA [13], BA [28], and AA [6] appears at 1652, 1625, and 1618 cm^{-1}, respectively. Therefore, it seems that this vibrational mode is strongly affected by the nature of the terminal groups. Electron withdrawing groups shifts the position of this mode of vibration towards higher frequencies. Similar behavior has been observed for C=O stretching in carbonyl compounds [37]. Upon deuteration a red shift of about a few wave numbers has been observed for all aforementioned compounds.

The very strong band at 1605 cm^{-1} is assigned to symmetric C=C–C=O stretching coupled strongly to the OH in-plane bending motion. Upon deuteration this band moves about 80 cm^{-1} towards lower frequencies. This frequency shift, which is accompanied by a great increase in the activity of the corresponding Raman band, is characteristic of the enol form of β-diketones [6,13,24,28]. It is noteworthy that in D_2TFBA symmetric C=C–C=O stretching is strongly coupled to 19a of phenyl group. As it is shown in Fig. 2, this coupling greatly increases the 19a intensity, which is in excellent agreement with the theoretical results.

By comparing the calculated and experimental Raman and IR intensities, the bands at 1575 and 1565 cm^{-1} are assigned to 8b mode of phenyl group for 2TFBA and 4TFBA, respectively. These bands are slightly coupled to some of the vibrations of the enol ring, such as C=C and C=O stretching motions.

By considering the theoretical calculation and comparing the vibrational spectra of TFBA and BA, the weak band at about 1474 cm^{-1} is assigned to ν_a O–C=C–C + 19b, which is coupled with OH and α–CH in-plane bending motions. Upon deuteration this band shifts to 1453 cm^{-1}. The calculated frequency shifts for 2TFBA and 4TFBA are 6 and 15 cm^{-1}, respectively.

The strong and relatively broad IR band at 1280 cm^{-1} is assigned to OH in-plane bending mode coupled to 14 mode of phenyl group. Disappearing of this bond upon deuteration confirms the assignment. The strong Raman band at 1250 cm^{-1} is assigned to the OH in-plane bending coupled to C–C and C–CF_3 stretching. Disappearing of these bands upon deuteration is in excellent agreement with the calculation results. Both relatively strong bands in the Raman spectrum of D_2TFBA at 1092 and 1036 cm^{-1} have OD in-plane bending character, which the former is coupled to 18a and νsCF_3 while the latter is coupled to νs C–C=C and 18a.

Three strong infrared bands at 1205, 1162, and 1116 cm^{-1} are assigned to the C–F stretching modes. According to the calculations, the first two bands are caused by asymmetric CF_3 stretching modes and the latter is due to the symmetric CF_3 stretching mode, which is strongly coupled with δCH, νC–O and 18b. As it is shown in Fig. 2, upon deuteration the position of the first two bands are not affected while the third band shifts considerably towards lower frequencies, 1092 cm^{-1}. This spectral behavior is in excellent agreement with the calculation predictions. The weak IR band at 1025 cm^{-1} and the strong Raman band at 1000 cm^{-1} are assigned to 18a and 12 of phenyl group, respectively.

4.3.4. Below 1000 cm^{-1}

In this region, we expect to observe the vibrational band frequencies due to the C–CF_3 stretching, in-plane and out-of plane bending, O–H and C–H out of plane bending, and phenyl and chelated rings in plane and out of plane deformational modes.

The medium and broad band at about 890 cm^{-1} is correlated with the theoretical band at 959 cm^{-1}, which has mostly the O–H out-of-plane bending character. Upon deuteration, this band disappears and a new band appears at about 680 cm^{-1}. The corresponding band in BA/D_2BA, AA/D_2AA, and TFAA/D_2TFAA appears at about 960/720, 950/707, and 893/672 cm^{-1}. These frequency shifts also support the following trend in the hydrogen bond strength:

BA > AA > TFBA > TFAA

The IR spectrum of TFBA shows a weak band at 896 cm^{-1}, which is assigned to the CCC in-plane bending mode, the corresponding band in BA and AA occurs at about 926 [28] and 930 cm^{-1} [6], respectively.

The two medium bands at 718 and 578 cm^{-1} in the IR spectrum of TFBA are assigned to the symmetric and asymmetric CF_3 deformation modes, respectively. The corresponding bands in the TFAA are observed at 728 and 584 cm^{-1} [13].

The strong Raman band at 616 cm^{-1} is attributed to one of the in-plane enol ring deformations. The corresponding bands in BA [28], AA [6], and TFAA appear at 672, 640, and 528 cm^{-1}, respectively. The position of this band in the enol form of β-diketones has been correlated to the hydrogen bond strength [24]. Therefore, the position of this band is also in excellent agreement with the other spectroscopic results.

The O···O stretching mode in the TFBA appears at about 303 cm^{-1}. The corresponding bands in BA, TFBA, and AA occur at 396, 366, and 264 cm^{-1}, respectively. These results also strongly support the aforementioned trend in the hydrogen bond strength.

By comparing the calculated IR and Raman band frequencies and intensities with the corresponding experimental results, there are several frequencies, such as frequency numbers 18, 26, 31, 32, 41, 44, and 55 that support the coexistence of 2TFBA and 4TFBA conformers in the sample.

5. Conclusion

The IR and Raman frequencies and relative intensities of the vibrational bands for 2TFBA and 4TFBA were calculated at the B3LYP/6-311G** level of theory and compared the results with those of BA, AA, and TFAA. The predicted frequencies and intensities were compared with the experimental data. Comparison of the vibrational spectra and structural parameters of TFBA with those of BA, AA, and TFAA reveal the following trend in the hydrogen bond strength:

BA > AA > TFBA > TFAA

The geometries of two possible chelated enol forms of TFBA along with the corresponding open structures are fully optimized at B3LYP (DFT) level of theory using 6-31G**, and 6-311++G** basis sets. The resulted ground state energies suggest a small difference between the stability of these two enol forms. According to the vibrational spectroscopy analysis, it was concluded that these two conformers coexist in comparable ratio in the sample, which confirms the theoretical results. Comparison the structural parameters implies that the hydrogen bond strength of TFBA lies between those of BA and TFAA. This results is also proves that substitution of CH_3 group with the CF_3 group reduces the strength of the hydrogen bond.

Acknowledgement

We are grateful to the University of Ferdowsi (Mashhad) for its support of this research. Y.A.W. gratefully acknowledges the financial support from the Natural Sciences and Engineering Research Council (NSERC) of Canada. WestGrid and C-HORSE have partially provided the necessary computational resources

References

[1] A.H. Lowery, C. George, P.D. Antonio, J. Karle, J. Am. Chem. Soc. 93 (1971) 6399.
[2] R.S. Brown, A.T. Nakashima, R.C. Haddon, J. Am. Chem. Soc. 101 (1979) 3175.
[3] J. Emsley, Struct. Bond. 57 (1984) 147.
[4] F. Hibbert, J. Emsley, Hydrogen Bonding and Chemical Reactivity, Advanced in Physical Chemistry, vol. 26, Academic Press, London, 1990, p. 255.
[5] R. Bose, M.Y. Antipin, D. Bläser, K.A. Lyssenko, K.A. Lessen, J. Phys. Chem. B 102 (1998) 8654.
[6] S.F. Tayyari, F. Milani-Nejad, Spectrochim. Acta Part A 56 (2000) 2679.
[7] A.L. Andreassen, D. Zebelman, S.H. Bauer, J. Am. Chem. Soc. 93 (1971) 1148.
[8] A.H. Lowry, C.G.P. D'Antonio, J. Karle, J. Am. Chem. Soc. 93 (1971) 6399.
[9] A. Camerman, D. Mostopaolo, N. Camerman, J. Am. Chem. Soc. 105 (1983) 1584.
[10] D.P. Tew, N.C. Handy, S. Carter, Mol. Phys. 102 (2004) 2217.
[11] K. Iijima, A. Onhogi, D. Shibata, J. Mol. Struct. 156 (1987) 111.
[12] R.D.G. Jones, Acta Crystallogr. B 32 (1976) 2133.
[13] M. Zahedi-Tabrizi, F. Tayyari, Z. Moosavi-Tekyeh, S.F. Tayyari, Spectrochim. Acta, in press.
[14] V.B. Delchev, G.S. Nikolov, Monatsh. Chem. 132 (2001) 339.
[15] S.F. Tayyari, F. Milani-Nejad, H. Rahemi, Spectrochim. Acta 58 (8) (2002) 1679.
[16] S.F. Tayyari, S. Salemi, M. Zahedi-Tabrizi, M. Behforouz, J. Mol. Struct. 694 (2004) 91.
[17] T. Chiavassa, P. Verlaque, L. Pizalla, P. Roubin, Spectrochim. Acta 50A (1993) 343.
[18] T. Chiavassa, P. Roubin, L. Pizalla, P. Verlaque, A. Allouche, F. Marinelli, J. Phys. Chem. 96 (1992) 659.
[19] G. Buemi, J. Mol. Struct. (Theochem.) 499 (2000) 21.
[20] V. Bertolasi, P. Gilli, V. Ferretti, G. Gilli, J. Am. Chem. Soc. 113 (1991) 4917.
[21] J. Tollec, in: Z. Rappoport (Ed.), The Chemistry of the Enols, John Wiley & Sons, New York, 1990, p. 366.
[22] R.L. Lintvedt, H.F. Holtzclaw Jr., Inorg. Chem. 5 (1966) 239.
[23] S.F. Tayyari, Th. Zeegers-Huyskens, J.L. Wood, Spectrochim. Acta 35A (1979) 1265.
[24] S.F. Tayyari, Th. Zeegers-Huyskens, J.L. Wood, Spectrochim. Acta 35A (1979) 1289.
[25] G.K.H. Madsen, B.B. Iversen, F.K. Larsen, M. Kapon, G.M. Reisner, F.H. Herbstein, J. Am. Chem. Soc. 120 (1998) 10040.
[26] B. Schiøtt, B. Bo, G.K.H. Iversen, F. Madsen, K. Larsen, T.C. Bruice, Proc. Natl. Acad. Sci. U.S.A. 95 (1998) 12799.
[27] M. Gorodetsky, Z. Luz, Y. Mazur, J. Am. Chem. Soc. 89 (1967) 1183.
[28] S.F. Tayyari, J.S. Emampour, M. Vakili, A. Nekoie, S. Salemi, H. Eshghi, M. Hassanpour, in press.
[29] D.C. Nonhebel, Tetrahedron 24 (1968) 1869.
[30] M.J. Frisch, G.W. Trucks, H.B. Schlegel, G.E. Scuseria, M.A. Robb, J.R. Cheeseman, J.A. Montgomery Jr., T. Reven, N. Kudin, J.C. Burant, J.M. Millam, S.S. Iyengar, J. Tomasi, V. Barone, B. Mennucci, M. Cossi, G. Scalmani, N. Rega, G.A. Petersson, H. Nakatsuji, M. Hada, M. Ehara, K. Toyota, R. Fukuda, J. Hasegawa, M. Ishida, T. Nakajima, Y. Honda, O. Kitao, H. Nakai, M. Klene, X. Li, J.E. Knox, H.P. Hratchian, J.B. Cross, C. Adamo, J. Jaramillo, R. Gomperts, R.E. Stratmann, O. Yazyev, A.J. Austin, R. Cammi, C. Pomelli, J.W. Ochterski, P.Y. Ayala, K. Morokuma, G.A. Voth, P. Salvador, J.J. Dannenberg, V.G. Zakrzewski, S. Dapprich, A.D. Daniels, M.C. Strain, O. Farkas, D.K. Malick, A.D. Rabuck, K. Raghavachari, J.B. Foresman, J.V. Ortiz, Q. Cui, A.G. Baboul, S. Clifford, J. Cioslowski, B.B. Stefanov, G. Liu, A. Liashenko, P. Piskorz, I. Komaromi, R.L. Martin, D.J. Fox, T. Keith, M.A. Al-Laham, C.Y. Peng, A. Nanayakkara, M. Challacombe, P.M.W. Gill, B. Johnson, W. Chen, M.W. Wong, C. Gonzalez, J.A. Pople, GAUSSIAN03, Revision B.05, Gaussian Inc., Pittsburgh PA, 2003.
[31] J.K. Badenhoop, A.E. Reed, J.E. Carpenter, J.A. Bohmann, C.M. Morales, F. Weinhold, E.D. Glendening, NBO 5.0, Theoretical Chemistry Institute, University of Wisconsin, Madison, 2001.
[32] A.D. Becke, J. Chem. Phys. 98 (1993) 5648.
[33] C. Lee, W. Yang, R.G. Parr, Phys. Rev. B 37 (1988) 785.
[34] K.W. Wiberg, Tetrahedron 24 (1968) 1083.
[35] A.E. Reed, L.A. Curtiss, F. Weinhold, Chem. Rev. 88 (1988) 899.
[36] E.B. Wilson, Phys. Rev. 4 (1934) 706.
[37] N.B. Colthup, L.H. Daly, S.E. Wiberley, Introduction to Infrared and Raman Spectroscopy, Academic Press Inc., 1975.
[38] D.N. Shigorin, M.M. Shemykin, M.N. Kolosov, Dokl. Akad. Nauk. SSSR 108 (1956) 672.
[39] D.N. Shigorin, E.A. Gastillovich, T.S. Kopteva, M.M. Victorova, Ah. Fiz. Khim. 42 (1968) 1231.